Renewable Energy 76 (2015) 318–329

Contents lists available at ScienceDirect

Renewable Energy

journal homepage: www.elsevier.com/locate/renene

Configurable, Hierarchical, Model-based, Scheduling Control with photovoltaic generators in power distribution circuits

Jaesung Jung [a, *], Ahmet Onen [b], Kevin Russell [c], Robert P. Broadwater [d], Steve Steffel [e], Alex Dinkel [e]

[a] Sustainable Energy Technologies Department, Brookhaven National Laboratory, Upton, NY, USA
[b] Department of Electrical and Electronics Engineering, Abdullah Gul University, Kayseri, Turkey
[c] Electrical Distribution Design, Inc., Blacksburg, VA, USA
[d] Department of Electrical and Computer Engineering, Virginia Polytechnic Institute and State University, Blacksburg, VA, USA
[e] Pepco Holdings, Inc., Washington, D.C., USA

ARTICLE INFO

Article history:
Received 2 January 2014
Accepted 16 November 2014
Available online 2 December 2014

Keywords:
Reactive power control
Hierarchical control
Local control
Power distribution control
PV integration
Aggregation PV

ABSTRACT

Existing distribution systems and their associated controls have been around for decades. Most distribution circuits have capacity to accommodate some level of PV generation, but the question is how much can they handle without creating problems. This paper proposes a Configurable, Hierarchical, Model-based, Scheduling Control (CHMSC) of automated utility control devices and photovoltaic (PV) generators. In the study here the automated control devices are assumed to be owned by the utility and the PV generators and PV generator controls by another party. The CHMSC, which exists in a hierarchical control architecture that is failure tolerant, strives to maintain the voltage level that existed before introducing the PV into the circuit while minimizing the circuit loss and reducing the motion of the automated control devices. This is accomplished using prioritized objectives. The CHMSC sends control signals to the local controllers of the automated control devices and PV controllers. To evaluate the performance of the CHMSC, increasing PV levels of adoption are analyzed in a model of an actual circuit that has significant existing PV penetration and automated voltage control devices. The CHMSC control performance is compared with that of existing, local control. Simulation results presented demonstrate that the CHMSC algorithm results in better voltage control, lower losses, and reduced automated control device motion, especially as the penetration level of PV increases.

Published by Elsevier Ltd.

1. Introduction

Photovoltaic (PV) generation is one of the most rapidly growing renewable energy sources, and is regarded as an appealing alternative to conventional power generated from fossil fuel. This has led to efforts to increase PV generation levels in the U.S. [1]. Although the integration of PV brings many advantages, high penetration of PV provides a number of challenges in power system operation, mainly due to its uncertain and intermittent nature.

A major research challenge is optimized control of high PV penetration within the existing power system. In a power distribution circuit that contains a high level of PV generation that is not combined with rapidly acting storage, a sudden change of PV generation can create voltage problems, which in turn may limit the amount of PV generation that can be added to the circuit.

A control algorithm that dispatches real and reactive PV generator power can be used to address this problem, keeping voltages and power factors at desired levels. PV generator control structures can be classified into three categories; local, hierarchical, and decentralized control [2–9]. In all of these control paradigms it is assumed that each PV generator has its own local controller.

Local PV generation inverter control is primarily used today, which aims to control PV operating points using local measurements. Local control is typically low cost and simple to operate and maintain. However, as PV penetration levels increase, it becomes more and more difficult to tune PV inverter and distribution circuit voltage control device settings to meet requirements. Also, with

* Corresponding author. Postal address: Brookhaven National Laboratory, Sustainable Energy Technologies Department, Bldg. 179B – P.O. Box 5000, Upton, NY 11973-5000 USA. Tel.: +1 631 344 2643.
E-mail address: jsjung@bnl.gov (J. Jung).

http://dx.doi.org/10.1016/j.renene.2014.11.046
0960-1481/Published by Elsevier Ltd.

local control only, it is difficult to handle the multitude of failure scenarios that are possible.

Here, hierarchical control collects circuit-wide information, and uses this big picture view to make supervisory level decisions that are used to better coordinate local device actions to meet system level objectives. Under this strategy, local control is still used to insure safety and to protect equipment from damage. If communications are lost between local controllers and the hierarchical control, the local control can continue to work similar to the control that is used today. An advantage of hierarchical control is that multi-objective optimization solutions can be achieved. If the hierarchical control is model based, then the control can handle all scenarios that are reflected in the model solution.

Many PV hierarchical control strategies are presented in Refs. [10–18]. In Refs. [10–12] reactive power injection of the PV is used to reduce voltage deviations caused by large PV penetrations. The control strategy minimizes circuit loss while maintaining the voltage within limits in Refs. [13–16]. An active curtailment strategy to reduce PV power injection is used to prevent voltage violations in Refs. [17,18]. Other work has investigated optimal coordination of control devices. In Refs. [19–22] different automated control devices are coordinated to find optimal dispatch schedules. Optimal control of the automated control devices is able to reduce circuit loss and improve the voltage profile [19–22]. In these papers different automated control devices are coordinated to find optimal dispatch schedules.

This paper introduces a hierarchical control algorithm referred to as Configurable, Hierarchical, Model-based Scheduling Control (CHMSC) for maintaining the average customer voltage profile obtained before introducing the PV into the circuit. The CHMSC control algorithm addresses optimal operation of automated devices and PV generators for voltage control and reactive power compensation, where stable system conditions are assumed. The CHMSC algorithm first looks at the operation of control devices owned by the utility, such as voltage regulators and switched capacitor banks, and uses time-series based simulation to determine a control schedule that works to minimize circuit loss while simultaneously reducing the motion of the automated control devices. This control schedule is created without considering PV generation. The CHMSC algorithm then generates coordinated PV inverter control set-points that work to maintain the system operating conditions established by the utility control devices. Thus, the CHMSC algorithm provides time varying set-points to local controllers for both the automated control devices and PV controllers.

The paper is organized as follows. Section 2 presents the CHMSC algorithm and its coordination. In Section 3 the proposed control is analyzed. Its effectiveness is shown by comparing the CHMSC performance with the performance of local control. Finally, findings of the study are summarized in Section 4.

2. Configurable, Hierarchical, Model-based, Scheduling Control

The main objective of CHMSC is to determine the optimum operating circuit voltage profiles and control schedule prior to introducing PV into the circuit, then use hierarchical PV controller set-point adjustment to help maintain this schedule as PV generated power is injected into the system. The approach reduces losses and voltage control device movement, while minimizing the impact that PV will have on circuit operation, which was most likely designed without any consideration given to installation of PV. CHMSC works to have the PV generation support the optimum voltage profiles and control schedule. The term optimum is associated here with discrete searches based upon the CHMSC prioritized objectives.

2.1. CHMSC outline

Circuit measurements are sent to a control center where CHMSC is located and makes decisions on control actions based on all measurements and the control objectives, as shown in Fig. 1. As illustrated in Fig. 1, optimum profiles determined by CHMSC are sent to automated control devices and PVs that have communications. CHMSC, using load and solar forecasts, will take into account the expected actions of control devices and PV generators that do not have communications and are controlled solely by their own local controller. Two such local controllers are illustrated in Fig. 1. The CHMSC control algorithm can be used on any distribution circuit topology, including radial, lightly meshed, and heavily meshed.

CHMSC calculates schedules as illustrated in Fig. 2. Using the load forecast, CHMSC first calculates the optimal schedules for the automated control devices in the absence of PV generation, referred to here as base controller schedule. The base controller schedule provides a time varying schedule for utility control devices and also optimum voltage schedules to be followed throughout the circuit. That is, the optimum voltage schedule varies from circuit location to circuit location. At a given circuit location, the optimum voltage schedule varies as a function of time. Next, using the solar forecast and the optimum voltage schedules, the optimal schedules for the PV generators are determined. The PV controller schedule provides

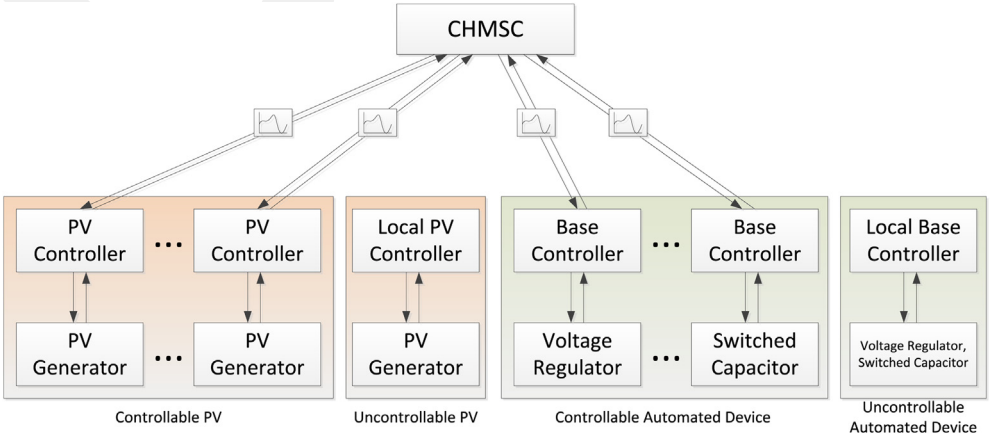

Fig. 1. Control system architecture.

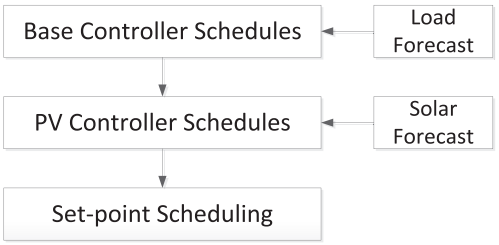

Fig. 2. CHMSC architecture.

a time varying power factor schedule for each PV controller. That is, each PV controller may have a different time varying power factor schedule. This is because in a large circuit different PV controllers may be operating at different system voltages and loading conditions. Then, based upon the set-point type required for each local controller, such as voltage, power factor, or other, optimal set-point schedules are determined and provided to individual local controllers, whether they be utility owned or not. Thus, the set-point schedules are time varying and vary from one local controller to another. The algorithms used to determine the base controller and PV controller schedules are presented in sections 2.2 and 2.3, respectively.

Based upon circuit and PV generation measurements, the CHMSC updates its calculations every 5 min. If the optimal set-point schedules for a base or PV controller have changed significantly from the ones currently being used, then the set-point schedules are updated for the local controllers. This update cycle is similar to that used in real-time energy markets [23].

If a PV generator is lost or a circuit reconfiguration occurs, the CHMSC immediately recalculates optimal schedules based upon the new situation. Note that if a communication failure occurs, the local controllers can continue to work against the optimal schedule previously provided as long as the variable being controlled, such as voltage, stays within the allowable range. If the locally measured variable goes out of bounds, then the local control will override the use of the optimal schedule.

2.2. Base controller schedule

Controller schedules represent the planned operation of the controllers over a period of time. Here the controller schedules are eventually determined in terms of control variable set-points, such as power factor or voltage set-points, as a function of time. However, in this section the schedules will initially be determined in terms of control device step positions.

The base controller schedules are determined by performing a search over controllable single-step (often switched shunt capacitors) and multi-step device (often voltage regulators) positions to find one or more sets of device positions that satisfy three prioritized objectives [20–22]. That is, there may be multiple control solutions that satisfy one or more of the objectives, where each control solution is represented by a set of device positions.

The highest priority control objective is to maintain the average customer voltage within a desired bandwidth of a set-point without violating voltage operating constraint limits. If more than one set of device positions satisfy the highest priority objective, the set with the smallest number of total device steps, or least device motion, is selected. If two or more sets of device positions satisfy the voltage criteria and have the same total device motion, then a set with the least circuit loss is selected.

A flowchart of the algorithm used for determining the base controller schedules is illustrated in Fig. 3. Let M_n represent the total number of allowable device steps at time n. M_n is related to the individual control device steps by

$$M_n = \sum_{k=1}^{K} m_{n,k} \tag{1}$$

where K is the total number of controllable devices and $m_{n,k}$ are the number of steps of device k at time n subject to the constraint

$$T_k^{\min} \le T_{n,k} \le T_k^{\max} \tag{2}$$

where $T_{n,k}$ is the step at time n, and $T_k^{\min}$ and $T_k^{\max}$ are the limits of the step position.

The first priority is to maintain the average customer voltage V_n within a range of a desired value $V_{\text{ref},n}$. This is the average customer voltage that would exist without PV generation in the circuit at time n. The voltage deviation is calculated by

$$\left|V_n - V_{\text{ref},n}\right| < V_{\text{tol},n} \tag{3}$$

where

$$V_n = \text{avg}\left(\sum v_{i,n}\right) \tag{4}$$

$V_{\text{tol},n}$ is the acceptable voltage deviation at time n

$v_{i,n}$ is the customer voltage of the component i at time n.

$V_{\text{tol},n}$ is defined as ±1% of the desired voltage ($V_{\text{ref},n}$) in this paper.

If any operating constraint limits are violated, such as

$$v_i^{\min} \le v_{i,n} \le v_i^{\max} \tag{5}$$

where $v_i^{\min}$ and $v_i^{\max}$ are lower and upper limits, respectively, on customer voltage, then the reference voltage is modified until either the constraint violation is eliminated or the controllers reach their limits. Note that the voltage control limits can change depending upon the type of customer.

If more than one control solution exists that satisfies the voltage criteria, then the second priority, minimize the steps taken by the control devices, is evaluated.

Finally, if more than one control solution exists which satisfies both the voltage and minimum controller motion criteria, the CHMSC algorithm works on the third priority, to reduce the circuit loss, where the circuit loss is calculated as

$$L_n = \sum \sqrt{P_{\text{Loss},i,n}^2 + Q_{\text{Loss},i,n}^2} \tag{6}$$

where $P_{\text{Loss},i,n}$ is the real power loss and $Q_{\text{Loss},i,n}$ is the reactive power loss of each component.

If a control solution that satisfies the highest priority is not acquired in M_n steps, the total allowable steps M_n is increased and the search repeated.

For each device k, a set of step positions $\{T_{n,k}\}$ as a function of time step n is thus determined, and this defines the schedule for device k in terms of actual step positions. Then, for each device k, a schedule of optimum voltage set-points $\{\text{Vop}_{n,k}\}$ is created. The optimum voltage schedules are then used in determining the optimum schedules for the PV generator controls, which is addressed in the next section.

2.3. PV controller schedule

The PV control algorithm uses an iterative approach to adjusting the power factors of the controllable PV to minimize the customer level voltage deviations from the optimum voltage profile obtained

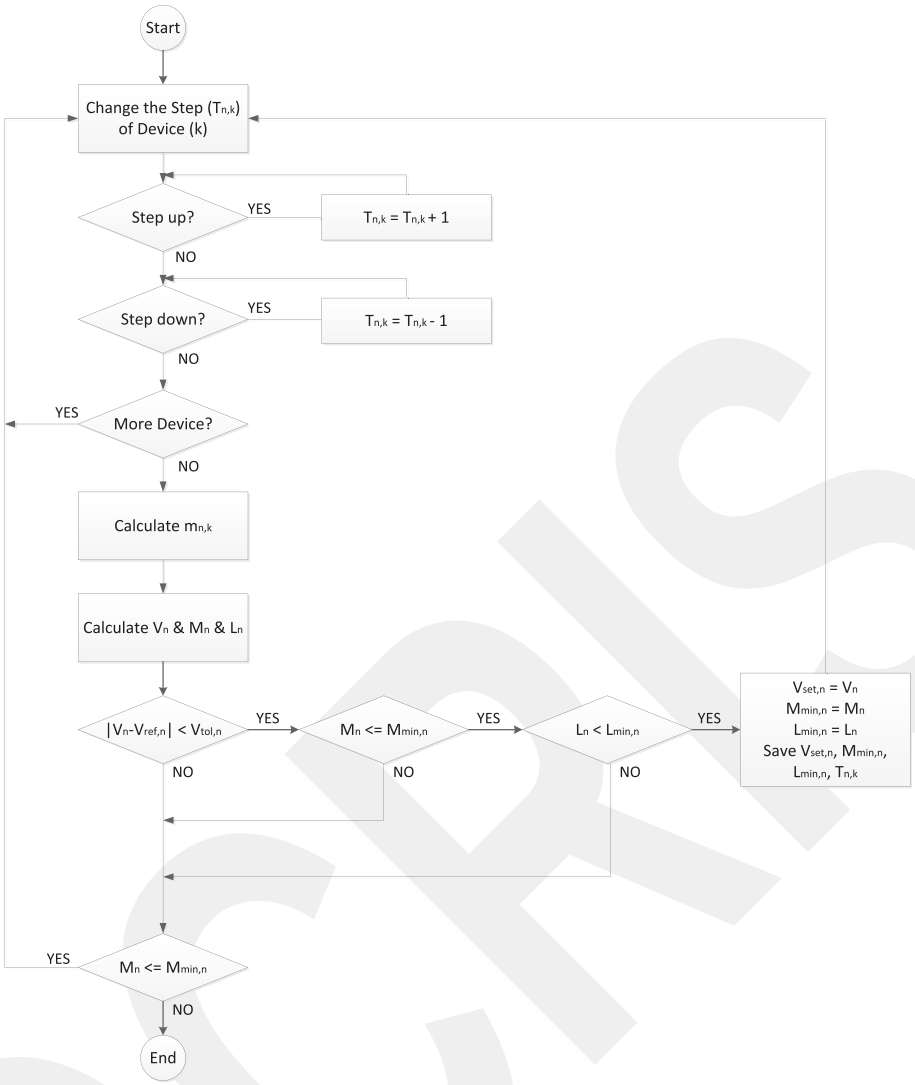

Fig. 3. Flowchart for base controller schedule.

from the base controller schedules, as illustrated in Fig. 4. Again note that for a given time point the voltage set-points determined in the base controller schedule may vary from PV generator to PV generator. Also, note that at different time points for a given PV generator the voltage set-point may vary.

If the optimum set-point is greater than the current voltage, the power factor is adjusted to supply reactive power. If the optimum set-point is less than the current voltage, the power factor is adjusted to consume reactive power. Discrete power factor steps are used by the algorithm. The algorithm first changes the power factor for a PV generator by increasing or decreasing the power factor in steps of 0.1. If the average customer voltage falls within ±0.5% of the optimum set-point, the algorithm changes the power factor by 0.01 steps with the following constraint:

$$PF_n^{min} \le PF_n \le PF_n^{max} \tag{7}$$

where PF = power factor.

After the power factors of all PVs are determined, the algorithm calculates the average customer voltage for the circuit (V_n). The objective is to reduce the voltage deviation from the optimum set-point ($V_{set,n}$) established by the automated control devices. Next the voltage deviation is compared with the saved minimum deviation ($dV_{min,n}$) as:

$$\left|V_n - V_{set,n}\right| < dV_{min,n} \tag{8}$$

If the algorithm finds a better power factor for the controller, it saves the results. The algorithm then returns to the start to change the power factor of the PV and begin a new iteration. One hundred iterations are used as the maximum in this work.

Individual local controllers may not work directly in terms of voltage and power factor set-points. Thus, the CHMSC controller finally performs set-point scheduling, as illustrated in Fig. 2, based upon the individual controller needs.

2.4. Local controller

For optimum operation, the optimum voltage and power factor schedules would be transmitted to all local controllers, as illustrated in Fig. 1, and all local controllers would work directly with the optimum schedules. However, most existing PV controllers are not designed to take such schedules. Here we will use a common PV local control scheme, but assume that the voltage set-point of the local PV controller can be varied.

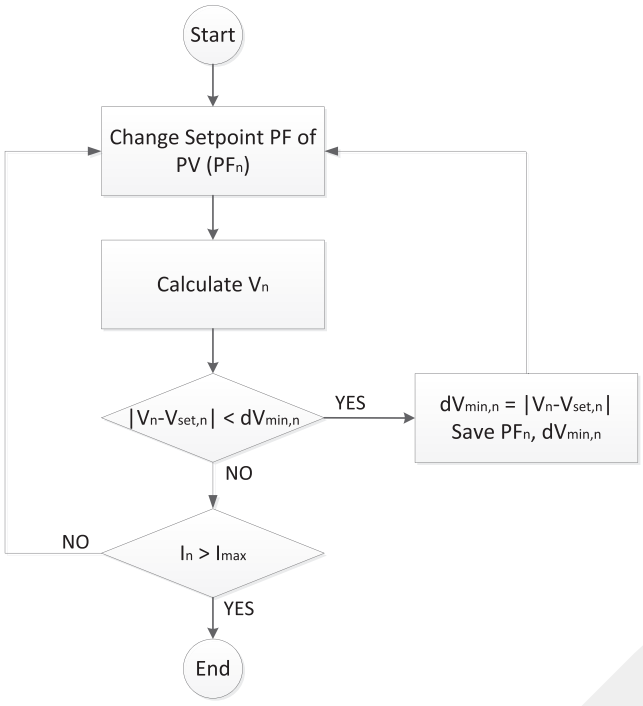

Fig. 4. Flowchart for PV controller schedule.

For local control of PVs, voltage-reactive power droop control is used in the work here, as shown in Fig. 5 [24]. This control provides voltage regulation support by supplying reactive power if the line voltage drops below the selected voltage set-point and by consuming reactive power if the line voltage is higher than the selected voltage set-point. The reactive power that can be supplied is limited, as illustrated in Fig. 5. Note that here the maximum reactive power is limited at 70% of the PV MVA rating. The gain used for the droop control is 2500 var/volt. This gain and the maximum reactive power limits are used for both the local control and CHMSC simulations described in the following sections. The major difference between the local control and the CHMSC control is that the voltage set-point to the local control changes with CHMSC and the set-point does not change when CHMSC is not used (i.e., the voltage set-point is fixed when just local control is used).

Utility control devices considered here are voltage regulators and switched shunt capacitors. Voltage regulators provide the output voltage to be regulated from 90% to 110%. For example, each step in a 32 multi-step voltage regulator having a 20% voltage range of regulation represents a 0.625% voltage change. Therefore, one step change of a voltage regulator is seen to result in a voltage change of 0.75 V based on a 120 V base.

Switched shunt capacitors are equipped with controllers that use local measurements to determine when to switch the capacitors on and off. For example, when the measured voltage is higher than the desired voltage, the controller opens the switch to remove the capacitor from service. When the voltage drops below the desired voltage, the controller closes the switch to place the capacitor in service.

3. Evaluation of Configurable, Hierarchical, Model-based, Scheduling Control

To evaluate the performance of the CHMSC, different PV adoption levels are analyzed. As more and more PVs are connected to the system the system behavior is affected. In this section the performance of CHMSC is compared with local control. When just local control is used, the voltage set-points are not updated.

3.1. Simulation study

The distribution circuit to be analyzed is shown in Fig. 6. The circuit model is derived from data for an actual circuit. It is a 13.2 kV, Y-connected circuit. The time varying customer loads are estimated from averaged hourly SCADA measurements, hourly customer kWh load data, and monthly kWh load data processed by load research statistics to create hourly loading estimates for each customer [25,26].

The circuit studied contains 21 voltage regulators and 8 switched shunt capacitors. The voltage regulators operate on voltage control with a 1.0 V bandwidth and ±16 steps. The switched shunt capacitors also operate to control voltage with specified turn on and turn off voltage limits.

This circuit has 4 existing PV generators, referred to as baseline generators, as marked in Fig. 6. The existing baseline PV generators are now controlled in the field to unity power factor and have 1 s resolution real power measurements available. Here the simulation uses these 1 s measurements in a quasi-steady state power flow. For the simulation of the higher PV penetrations, 1 MW PV generators are used. The generation from the added PV generators considered in cases 1 and 2 is based on the baseline PV generator measurements. The locations of the added PV generators were randomly selected [27,28].

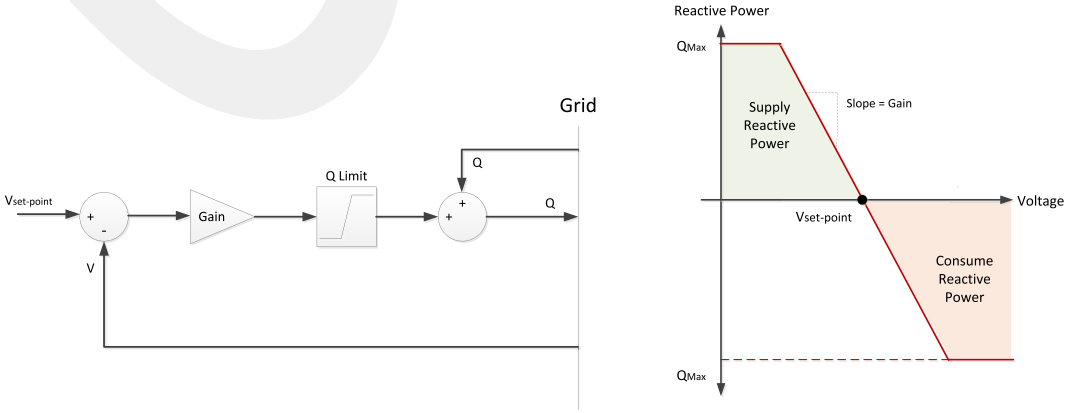

(a) voltage-reactive power control block diagram (b) voltage-reactive power characteristics

Fig. 5. Voltage–reactive power droop control.

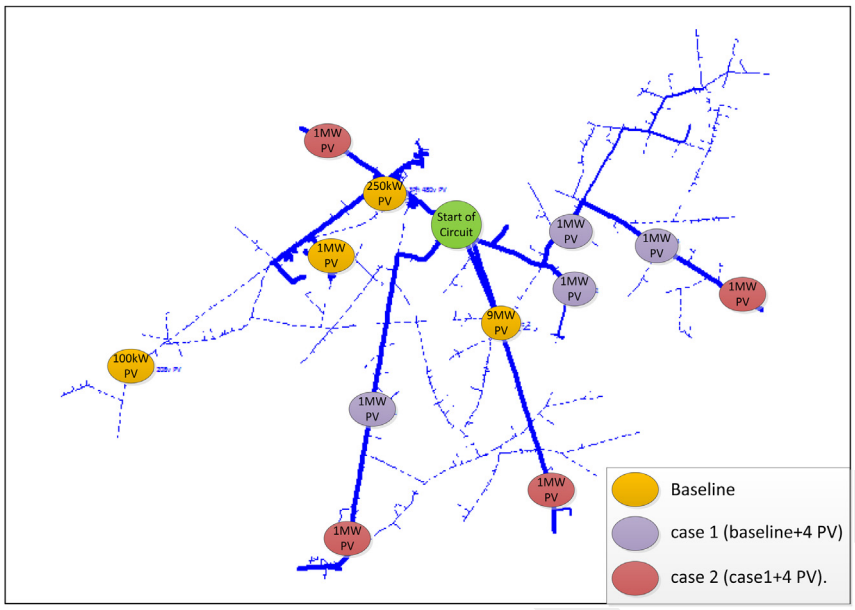

Fig. 6. Distribution circuit to be analyzed with baseline, case 1, and case 2 PV penetration levels.

April 2 from 14:00 to 16:00 contains the time of maximum PV generation for the existing generation, or baseline. This 2 h time period is used in the case studies to be presented. The PV generation data for the 9 MW PV on April 2 from 14:00 to 16:00 is shown in Fig. 7. In this paper 3 levels of PV penetration are analyzed and used in the controller comparisons, as indicated in Fig. 6: baseline case with existing generation; case 1 (baseline + four 1 MW PVs added to the circuit); and case 2 (case1 + four 1 MW PVs added to the circuit). The rated PV generation for the baseline case is 10.35 MW, for case 1, 14.35 MW, and for case 2, 18.35 MW.

The PV penetration percentage is calculated based on the following equation:

$$\text{PV penetration } (\%) = \frac{\text{Max PV generation}}{\text{Native load at max PV generation time}} \tag{9}$$

Thus, the definition of PV penetration used in this paper varies based on the selected time duration. The PV penetration for the selected day for analysis is approximately 69%, 96%, and 123% for the baseline case, case 1, and case 2, respectively.

High PV penetration often leads to reverse power flow conditions in distribution circuits. Bidirectional power flow can be detrimental to the performance of automated control devices. Fig. 8 shows the reverse power flow by circuit color on April 2 at 14:00 for the baseline. For case 2, representing a PV penetration level of 123%, the entire circuit would be colored with the reverse power flow (not shown in Fig. 8).

In order to evaluate control performance, PV generation changes are considered at the time of maximum PV generation [29]. For the baseline, Fig. 9 illustrates how voltage variations are observed as a function of loss of PV generation. From the figure it may be seen that a 1% voltage variation, based on a 120 V volt base, is observed when 20% of the PV generation is lost, where the generation loss occurs at maximum generation. Since one of the objectives here is to control the voltage variation to within 1%, the CHMSC will be re-run when a 20% variation of PV generation is observed. In Fig. 7 there are four times at which the PV generation varies more than

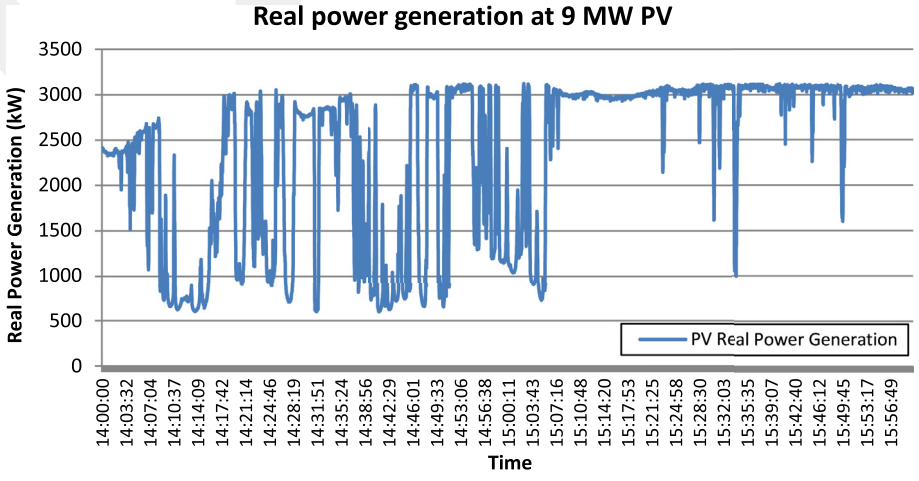

Fig. 7. Real power generation data at 9 MW PV on April 2 from 14:00 to 16:00.

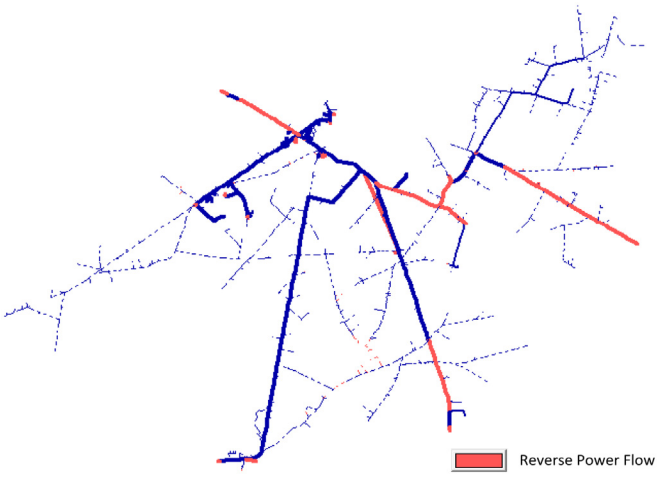

Fig. 8. Reverse power flow on April 2 at 14:00 corresponding to case 2.

20%, which are: 2:48:13 PM, 2:48:14 PM, 2:51:00 PM, 2:51:16 PM. Furthermore, in the CHMSC simulations the loss of communication is also tested at 2:25:00 PM and 3:55:00 PM.

When local control is not coordinated by CHMSC, the local control uses the nominal voltage as a set-point. Here the local PV controllers are modeled in Matlab, and then Matlab coder is used to convert the Matlab file to a dynamic link library file that is used in the power system simulation [30].

3.2. Comparison between local control and CHMSC for case 1

In this section the CHMSC simulation results are compared with the results of local control for case 1. Case 1 includes the existing 4 PV generation sites and 4 additional 1 MW PV generation sites, representing a PV penetration of 96%, as illustrated in Fig. 6. Five variables are used here in comparing CHMSC with local control, which are average customer voltage, circuit losses, steps of automated control devices, PV reactive power generation, and the voltage variation at the 9 MW PV generator.

3.2.1. Average customer voltage

Fig. 10 shows the optimal average customer voltage as a function of time obtained from CHMSC. In CHMSC the average customer voltage is calculated to reduce the circuit loss and minimize the automated control device motion. Actual optimal voltage set-points for PV generators will vary from PV generator to PV generator. Here the optimal set-points are updated every 5 min or when 20% changes in PV generation are observed. In Fig. 10, the optimal average customer voltage is shown at which the PV generation varies more than 20% and when the simulated loss of communication occurs.

Fig. 11 compares the average customer voltage obtained from CHMSC with that obtained from local control. From the figure both CHMSC and the local control maintain the average customer voltage within allowable ranges. However, as will be shown below, local control is not able to maintain voltages at specific locations within the allowable range.

3.2.2. Circuit loss

Figs. 12 and 13 show the real and reactive circuit loss comparisons, respectively. Both the real and reactive circuit losses are significantly reduced with CHMSC. Circuit loss summaries are shown in Table 1. For the 2 h simulation CHMSC is able to improve the real and reactive power loss over the local control by 38.06% and 45.83%, respectively.

3.2.3. PV reactive power generation

Fig. 14 show the reactive power generation at the largest PV generator, the 9 MW generator. Note that in all local control the maximum reactive power is limited at 70% of the PV MVA rating. As shown in Fig. 14, at the 9 MW generator the local control is always limited at the maximum reactive power injection. The CHMSC controls the reactive power to maintain the optimal voltage set-point, which is shown in the next section where the voltage variation is considered. With CHMSC the reactive power generation never reaches its limit. This is due to the participation of the other coordinated generators in the reactive power control.

3.2.4. Voltage variation

Figs. 15 and 16 show the primary system voltage variations with local control and CHMSC, respectively, at the 9 MW generator. The local control is not able to maintain the voltage set-point within the 1% variation limits because the reactive power generation is clamped at its limit. However, the CHMSC is able to maintain the voltage within the allowable range due to the coordination with other generators.

3.2.5. Steps of automated control devices

One of the CHMSC control objectives is to minimize the steps of the automated control devices themselves. The circuit studied has 21 voltage regulators and 8 switched shunt capacitors. Table 2 provides a summary of the control device steps and compares the local control with CHMSC for the 2 h simulation period. From the

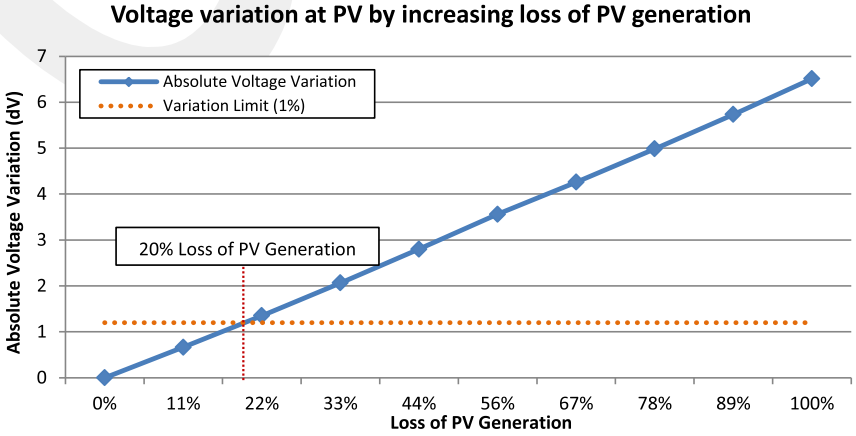

Fig. 9. Voltage variations by increasing levels of loss of generation for baseline condition.

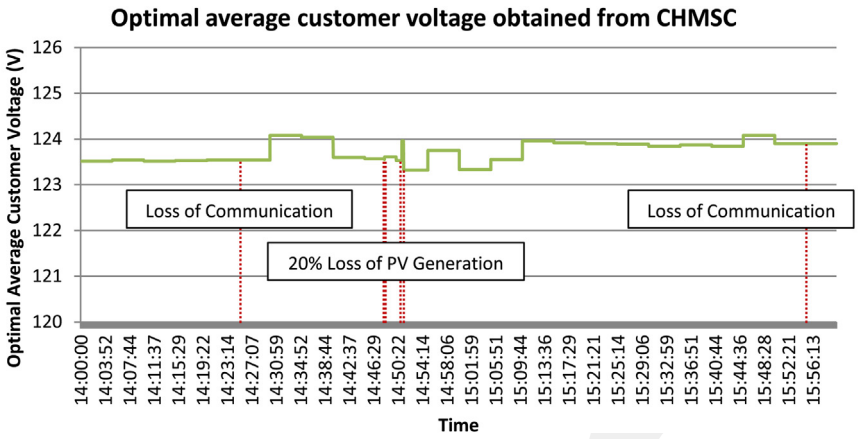

Fig. 10. CHMSC optimal average customer voltage.

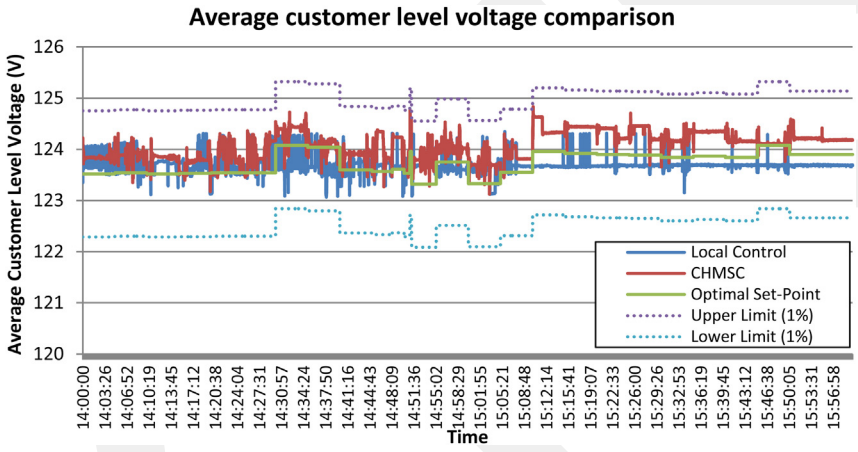

Fig. 11. Average customer level voltage comparison between local control and CHMSC for case 1.

table it may be seen that the CHMSC results in significantly fewer steps than local control.

3.3. Control performance comparisons for baseline, case 1, and case 2

In this section further comparisons of CHMSC with local control are presented for the baseline case, case 1, and case 2, where the cases are illustrated in Fig. 6. Circuit losses, automated device motion, voltage violations, and overload violations will be considered.

3.3.1. Circuit loss

Figs. 17 and 18 compares total real and reactive power losses as the level of PV generation increases from the baseline case to case 2.

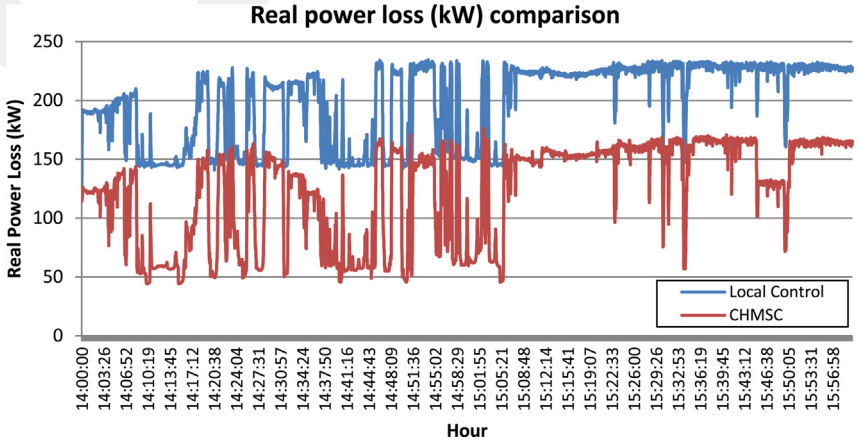

Fig. 12. Real power loss (kW) comparison between local control and CHMSC for case 1.

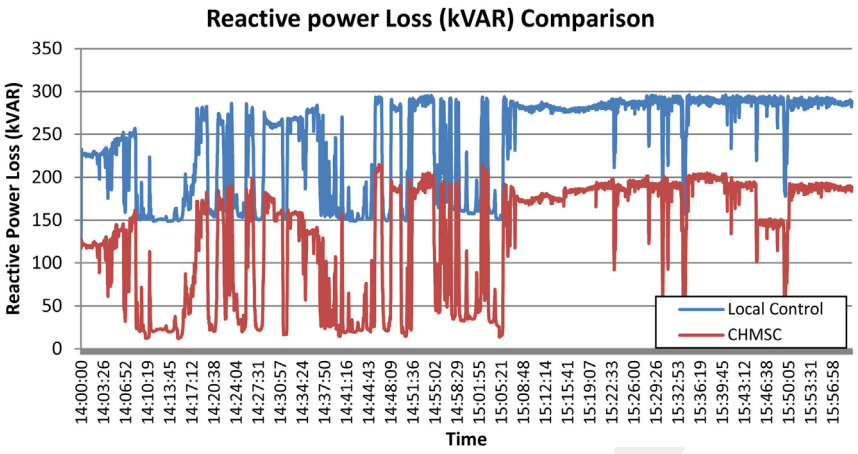

Fig. 13. Reacitve power loss (kVAR) comparison between local control and CHMSC for case 1.

Table 1
Comparison of the total circuit losses between local control and CHMSC for case 1.

	Local control	CHMSC	Improvement
Real power loss (kW-hr)	198.98 kW-hr	123.25 kW-hr	38.06%
Reactive power loss (kVAR-hr)	240.69 kVar-hr	130.38 kVar-hr	45.83%

Both real and reactive circuit losses increase with increasing PV generation, but in all cases CHMSC has significantly lower losses.

3.3.2. *Steps of automated control devices*

Fig. 19 compares the control motion, in terms of percent reduction of CHMSC over local control, as the level of PV

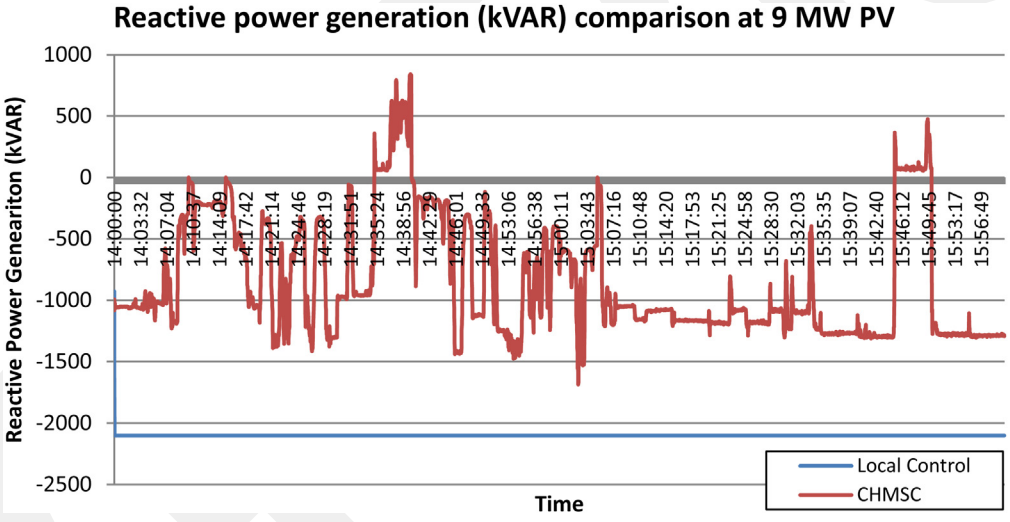

Fig. 14. Reactive power generation (kVAR) comparison at 9 MW PV between local control and CHMSC for case 1.

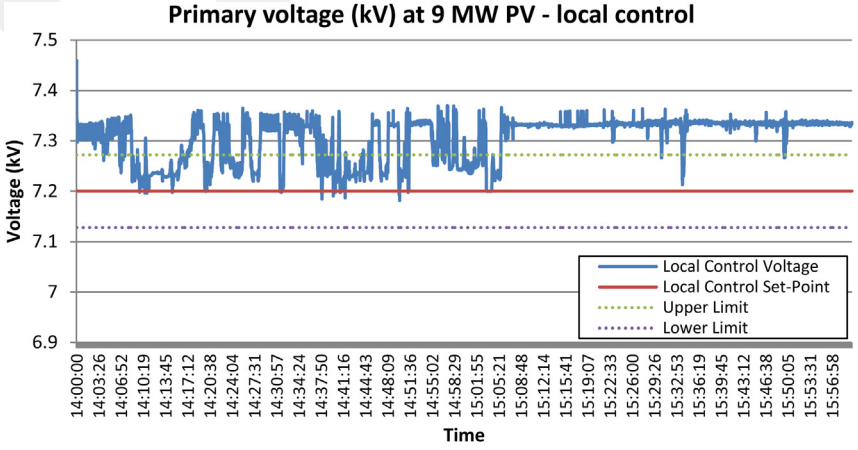

Fig. 15. Voltage at 9 MW PV using local control for case 1.

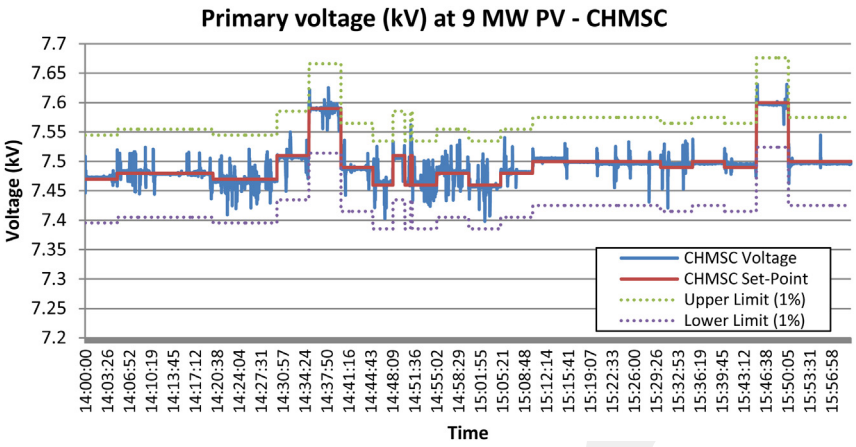

Fig. 16. Voltage at 9 MW PV using CHMSC for case 1.

Table 2
Total steps comparison of automated control devices for 2 h between local control and CHMSC for case 1.

	Local control	CHMSC	% Reduction in controller motion with CHMSC
All voltage regulators	2374	1559	34%
All switched shunt capacitors	1070	684	36%

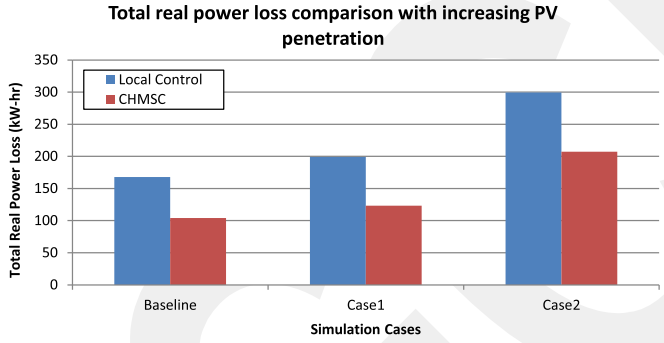

Fig. 17. Total real power loss comparison for 2 h simulation by increasing PV penetration.

penetration increases. As shown in the figure, the percent reduction ranges from a little over 20% to over 40%. And, as the PV penetration level increases, the improvement of CHMSC over local control continues to increase. It may be noted that CHMSC has a slightly larger improvement for switched capacitors.

3.3.3. Number of voltage violation

Fig. 20 shows how the number of customer voltage violations, low and high, increase as the level of PV generation increases. It may be noted that local control has more than four times the violations of CHMSC. Customer voltage violations are only reported at load busses, and there are 1109 load busses in the model. Since there are 7200 power flow runs performed over the 2 h period, there are 7,984,800 voltage calculations (7200 × 1109) that are checked for low or high voltage at load busses during the simulation. Hence, approximately 1600 voltage violations (worst case in Fig. 20) represent approximately 0.02% violations.

3.3.4. Number of overloading violation

Fig. 21 shows how the number of overloads increases as the level of PV generation increases. CHMSC has 93% and 54% fewer overloads for cases 1 and 2, respectively. An overload violation occurs when the power flow through a component exceeds the power rating of the component. Note that the circuit has 4883 components. Thus, there are 35,157,600 calculations (4883 × 7200) that are checked at individual components for an overload condition during the

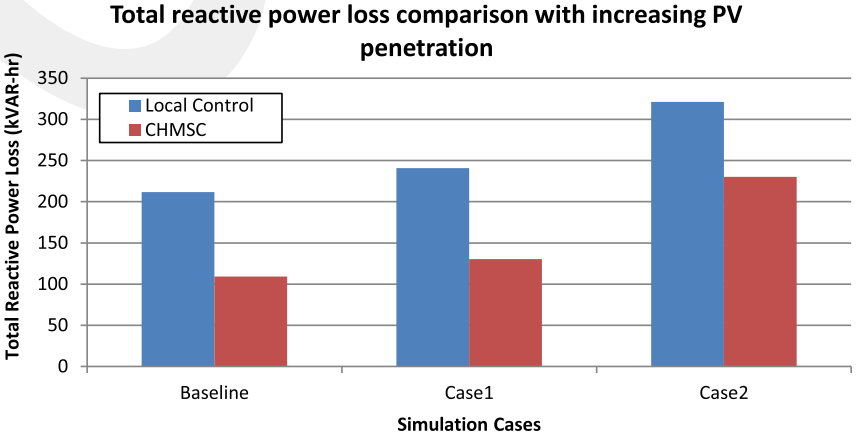

Fig. 18. Total reactive power loss comparison for 2 h simulation by increasing PV penetration.

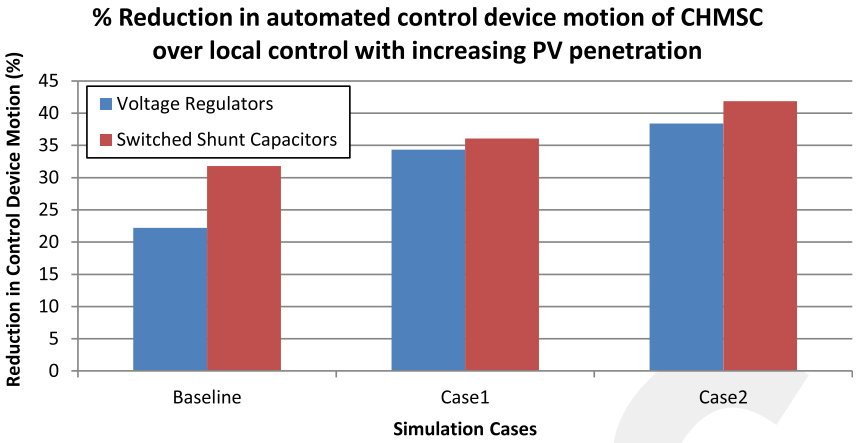

Fig. 19. Reduction in control device movement with CHMSC with increasing PV penetration.

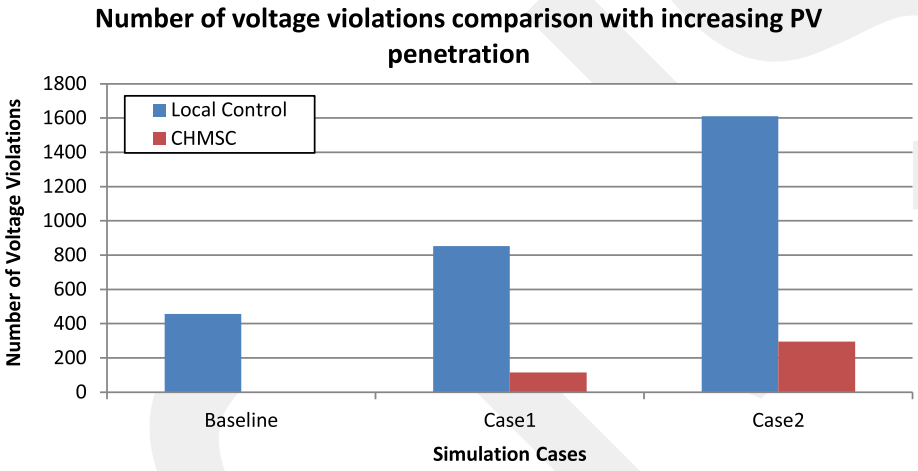

Fig. 20. Number of voltage violations during 2 h period with increasing PV penetration.

simulation. Hence, approximately 15,500 overload violations (worst case in Fig. 21) represent approximately 0.044% violations.

4. Conclusions

The Configurable, Hierarchical, Model-based, Scheduling Control presented uses utility automated control devices to establish an optimum voltage schedule, where the optimum voltage schedule varies with time-of-day and with circuit location. The optimum voltage schedule calculation does not consider PV generation. PV generators that have communications are then requested to help maintain the optimal voltage schedule. If a PV generator controller does not have communications, then CHMSC studies can be used to help determine

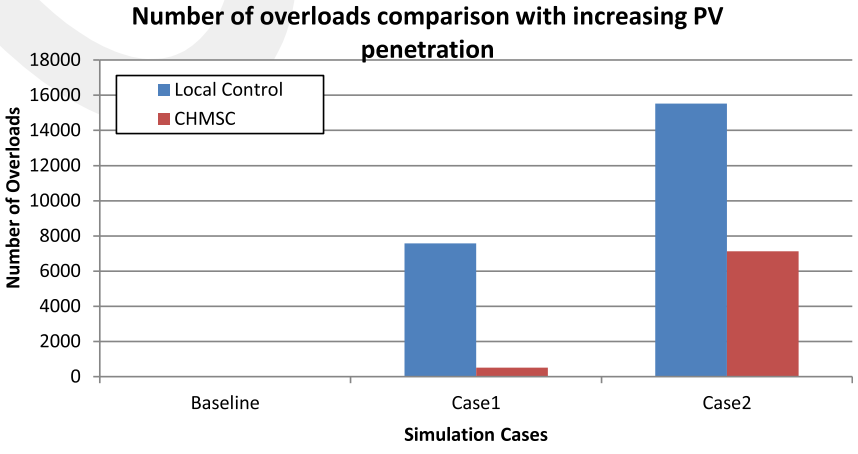

Fig. 21. Number of overloads during 2 h period with increasing PV penetration.

reasonable PV controller gains that support the power system operation.

A model of an existing circuit with high PV penetration (69%) was used as a starting point for the comparison of CHMSC with local control only. In performing the analysis 1 s PV generation measurement data from the existing solar generators was used. In the comparison CHMSC used the same local controllers, but varied the voltage set-points of the local controllers. The comparison of the performance between CHMSC and local control only was performed for three levels of PV penetration – 69%, 96%, and 123%. Comparisons included real losses, reactive losses, voltage violations, overload violations, motion of utility owned automated control devices, and the control of voltage. The CHMSC outperformed the local control only, and often the difference in performance increased as the level of PV penetration increased.

Existing distribution systems and their associated controls have been around for decades. Most distribution circuits have capacity to accommodate some level of PV generation, but the question is how much can they handle without creating problems. The control approach presented seeks to accommodate very high levels of PV penetration with the least impact on the system operation.

In this paper the CHMSC updates its calculations every 5 min or when PV generation has changed significantly. It is also necessary to control PV generation appropriately in dynamic events such as short circuits. Additional research concerning PV control in such emergency situations will be addressed in future work.

Acknowledgment

The authors would like to thank Pepco Holdings, Inc. and Electrical Distribution Design, Inc. for providing data, funding, and technical assistance used in this study.

References

[1] United States Department of Energy. SunShot vison study. Report DOE/GO-102012–3037. Feb. 2012. Available from:, http://www1.eere.energy.gov/solar/sunshot/vision_study.html.
[2] Zamora R, Srivastava AK. Controls for microgrids with storage: review, challenges, and research needs. Renew Sust Energy Rev 2010;14:2009–18.
[3] Planas E, Gil-de-Muro A, Andreu J, Kortabarria I, Alegria IM. General aspects, hierarchical controls and droop methods in microgrids: a review. Renew Sust Energy Rev 2013;17:147–59.
[4] Pandey SK, Mohanty SR, Kishor N. A literature survey on load-frequency control for conventional and distribution generation power systems. Renew Sust Energy Rev 2013;25:318–34.
[5] Nehrir MH, Wang C, Strunz K, Aki H, Ramakumar R, Bing J, et al. A review of hybrid renewable/alternative energy systems for electric power generation: configurations, control, and applications. IEEE Trans Sustain Energy 2011;2:392–403.
[6] Carmeli MS, Castelli-Dezza F, Mauri M, Marchegiani G, Rosati D. Control strategies and configurations of hybrid distributed generation systems. Renew Energy 2012;41:294–305.
[7] Lagorse J, Paire D, Miraoui A. A multi-agent system for energy management of distributed power sources. Renew Energy 2010;35:174–82.
[8] Dakkak M, Hirata A, Muhida R, Kawasaki Z. Operation strategy of residential centralized photovoltaic system in remote areas. Renew Energy 2003;28:997–1012.
[9] Xin H, Qu Z, Seuss J, Maknouninejad A. A self-organizing strategy for power flow control of photovoltaic generators in a distribution network 2011;26:1462–73.
[10] Miyamoto Y, Hayashi Y. Evaluation of generation efficiency and voltage deviation in residential clustered PV voltage control. In: 2011 37th IEEE photovoltaic specialists conference, Seattle, WA, USA; 2011.
[11] Carvalho PMS, Correia PF, Ferreira LAFM. Distributed reactive power generation control for voltage rise mitigation in distribution networks. IEEE Trans Power Syst 2008;23:766–72.
[12] Vovos PN, Kiprakis AE, Wallace AR, Harrison GP. Centralized and distributed voltage control: impact on distributed generation penetration. IEEE Trans Power Syst 2007;22:476–83.
[13] Liu X, Aichhorn A, Liu L, Li H. Coordinated control of distributed energy storage system with tap changer transformers for voltage rise mitigation under high photovoltaic penetration. IEEE Trans Smart Grid 2012;3:897–906.
[14] Hong Y-Y, Luo Y-F. Optimal VAR control considering wind farms using probabilistic load-flow and gray-based genetic algorithms. IEEE Trans Power Del 2009;24:1441–9.
[15] Carnano A, Torelli F, Alfonzetti F, Tuglie ED. Can PV plants provide a reactive power ancillary service? A treat offered by an on-line controller. Renew Energy 2011;36:1047–52.
[16] Niknam T. A new HBMO algorithm for multiobjective daily volt/var control in distribution systems considering distributed generators. Appl Energy 2011;88:778–88.
[17] Wang Y, Zhang P, Li W, Xiao W, Abdollahi A. Online overvoltage prevention control of photovoltaic generators in microgrids. IEEE Trans Smart Grid 2012;3:2071–8.
[18] Lin C-H, Hsieh W-L, Chen C-S, Hsu C-T, Ku T-T. Optimization of photovoltaic penetration in distribution systems considering annual duration curve of solar irradiation. IEEE Trans Power Syst 2012;27:1090–7.
[19] Park J-Y, Nam S-R, Park J-K. Control of a ULTC considering the dispatch schedule of capacitors in a distribution system. IEEE Trans Power Syst 2007;22:755–61.
[20] Hambrick J, Broadwater RP. Configurable, hierarchical, model-based control of electrical distribution circuits. IEEE Trans Power Syst 2011;26:1072–9.
[21] Onen A, Cheng D, Arghandeh R, Jung J, Woyak J, Dilek M, et al. Smart model based coordinated control based on feeder losses, energy consumption, and voltage violations. Elec Power Comp Syst 2013;41:1686–96.
[22] Jung J, Onen A, Arghandeh R, Broadwater RP. Coordinated control of automated devices and photovoltaic generators for voltage rise mitigation in power distribution circuits 2014;66:532–40.
[23] Ott AL. Experience with PJM market operation, system design, and implementation. IEEE Trans Power Syst 2003;18:528–34.
[24] Alatrash H, Amarin RA, Lam C. Enabling large-scale PV integration into the grid. In: 2012 IEEE green technologies conference, Tulsa, OK, USA; 2012.
[25] Broadwater RP, Sargent A, Yarali A, Shaalan HE, Nazarko J. Estimating substation peaks from load research data. IEEE Trans Power Del 1997;12:451–6.
[26] Sargent A, Broadwater RP, Thompson JC, Nazarko J. Estimation of diversity and KWHR-to-peak-KW factors from load research data 1994;9:1450–6.
[27] Jung J, Asgeirsson H, Basso T, Hambrick J, Dilek M, Seguin R, et al. Evaluation of DER adoption in the presence of new load growth and energy storage technologies. In: 2011 IEEE PES general meeting, Detroit, Michigan, USA; 2011.
[28] Jung J, Cho Y, Cheng D, Onen A, Arghandeh R, Dilek M, et al. Monte Carlo analysis of plug-in hybrid vehicles and distributed energy resource growth with residential energy storage in Michigan 2013;108:218–35.
[29] Eftekharnejad S, Vittal V, Heydt GT, Keel B, Loehr J. Impact of increase penetration of photovoltaic generation on power systems 2013;28:893–901.
[30] Matlab coder. Available from: http://www.mathworks.com/products/matlab-coder/.